BeBeC-2022-D10

AN EXTENDED SODIX METHOD FOR THE DIRECTIVITY ANALYSIS OF AIRFLOW NOISE SOURCE

Jianxin Lian*, Weiyang Qiao*, Weijie Chen, Kangshen Xiang, and Haojie Liu
School of Power and Energy, Northwestern Polytechnical University
West Youyi Road 127#, 710072, Xi'an, China

ABSTRACT

The aeroengine noise has a very strong directivity, and the directivity of sound source cannot be measured by traditional beamforming of the microphone array. SODIX, which was firstly proposed by Prof. Michel in DLR, is a deconvolution processing method of microphone array specially used for engine noise directivity identification and quantification. In order to overcomes the unstable calculation and long calculation time in SODIX, a new extended SODIX method – SODIX-Bes for sound source directivity identification and quantification is developed in this paper. In SODIX-Bes, the sound source position and spectrum in the flow field are firstly obtained by beamforming technology, and then the directivity and intensity of each sound source are identified by fitting the simulated sound source cross power spectrum with the test cross power spectrum of array. The computational simulation results show that the error of the SODIX-Bes method is less than 0.17 dB. A linear array with 31 microphones was designed to identify and analyse the leading-edge noise directivity and leading-edge noise reduction with wavy configuration for NACA65(12)-10 blade. The experimentally results show that SODIX-Bes is reliable and effective.

1 INTRODUCTION

The microphone array was first proposed by the British scientist Billingsley[1] in 1974. In 1976, Billingsley and Kinns[2] applied the microphone array technology to the measurement of engine aerodynamic noise, which was the first application of the microphone array measurement technology in aeroengine. From Billingsley's pioneering work to now, modern microphone array has been widely used in the research of aircraft/engine aerodynamic noise, and has been further extended to the research of high-speed train noise and modern automobile noise.

The traditional beamforming result of microphone array is the calculation result of point spread function convolution for point sound source. However, in fact, it is difficult to accurately determine the amplitude of the distributed sound source from the beamforming results, which often requires the user's personal experience[3,4]. In 1998, Dougherty and Stoker[5] first applied the deconvolution algorithm in the field of radio astronomy to data processing of the microphone array, they only calculated the point spread function of the strongest source in data processing, and continuously eliminated the influence of sidelobe from beamforming maps. After that, the microphone array deconvolution algorithms have

* Correspondence: qiaowy@nwpu.edu.cn; lianjianxin@mail.nwpu.edu.cn; Tel.: +86-13709183956

been rapidly developed, the most famous deconvolution algorithm is the DAMAS algorithm proposed and developed by Brooks and Humphreys[6,7,8] in 2004, which is the most important deconvolution algorithm in the acoustic measurement of the microphone array. Because the original algorithm of DAMAS requires a very high computational resource, two fast algorithms, DAMAS 2 and DAMAS 3, were further developed by Dougherty[9] in 2005. Another mature and accurate deconvolution algorithm is the Clean-SC (CLEAN based on spatial source coherence) method developed by Sijtsma[10]. At present, CLEAN-SC[10] and DAMAS[9] algorithms have been widely used in aero-acoustics and become standard deconvolution algorithms.

It is well known that, due to the working characteristics of the jet aeroengine, aeroengine noise is always radiated from the its inlet and outlet, and the noise radiation from the inlet and outlet of aeroengine has a strong directivity. However, the conventional microphone array is usually unable to identify the directivity of the sound source, it can only identify an average noise strength from the sound source to the direction of the centre of the microphone array. For the noise source with obvious directivity, simple beamforming of the microphone array can't accurately obtain the directivity and strength of the noise source.

In 1984, the directivity was analyzed in aircraft flyovers by Howell[11]. Miche et al.[12] tried to use the microphone array to measure the directivity of the sound source in 1999, They identified the noise source of the aircraft flying overhead, and measured the directivity of the noise source of the aircraft according to the change of the relative angle between the aircraft sound source and the array. In 2001, Siller and Michel[13] further extended this idea to the directivity experiment of the stationary sound source on the ground, they proposed a moving array measurement method to measure the directivity of engine inlet and outlet noise sources. For the moving sound source, this method is an effective measurement method, but for stationary sound sources on the ground, this method (moving array) is obviously a limited measurement method.

In order to solve the above technical problems of aeroengine noise source directivity identification, Michel et al.[14,15] firstly proposed a new inverse method of aeroengine noise source directivity experiment in 2008, and it is called as SODIX method (Source directivity modelling in cross-spectral matrix). SODIX is a data processing method based on directivity fitting of different sound sources, it extended the Blacodon and Elias[16,17] method to the directivity of sound sources. Since 2010, the SODIX has been further developed in DLR to improve its prediction accuracy and calculation efficiency [18,19,20]. In 2021, Sarradj extends the SODIX method to calculate a discrete directivity pattern of a rotating sound source[21].

But SODIX adopts the cross-spectrum matrix fitting of the full array microphone signal, thus forming a complex and huge set of nonlinear algebraic equations to solve. In particular, due to the cross-spectrum matrix of the full array microphone signal, SODIX contains the cross spectrum of the microphone signal with large separation distance and poor correlation, which further brings the solving stability problem.

In order to reduce the computational complexity of SODIX method and reduce the computation time, this paper proposes a new sound source directivity recognition method – SODIX-Bes (Source directivity modelling in cross-spectral matrix based on Beamforming Source), and the corresponding program was developed. This method takes advantage of the beamforming to accurately identify the sound source position and spectrum, and combined with SODIX method to identify the directivity of the sound source. The SODIX-Bes is described in section II of this paper. The section III uses computer simulation technology to simulate and verify the SODIX-Bes. The section IV uses the SODIX-Bes to study the leading-edge noise reduction of the NACA65(12)-10 blade with wavy leading-edge in a semi-anechoic chamber.

2 THE SODIX-BES METHOD

2.1 SODIX method

The cross-spectral matrix ($C_{m.n}^{mes}$) of measured signals is compared with a modelled matrix consisting of the sum of the matrices generated by each of the J unknown sources. The model cross-spectral matrix containing the directionality of the source

$$C_{m,n}^{\text{mod}} = \sum_{j=1}^{J} g_{m,j} D_{m,j} D_{n,j} g_{n,j}^{*} \tag{1}$$

Where $D_{m,j}$ is the directivity of the source intensity of source j toward microphone m.

$$g_{m,j} = e^{ikR_{m,j}} / R_{m,j} \tag{2}$$

Where $R_{m,i}$ is the distance from the microphone m to the sound source j, k=2$\pi f/c$.

The goal of SODIX is to determine the $D_{m,j}$ of source j toward microphone m such that the mean square error $F(D)$ between the measured and the modelled matrix becomes a minimum.

$$F(D) = \sum_{m,n}^{M} \left| C_{m,n}^{mes} - \sum_{j=1}^{J} g_{m,j} D_{m,j} D_{n,j} g_{n,j}^{*} \right|^2 \qquad (m,n = 1,2,...,M) \tag{3}$$

The minimum of $F(D)$ is obtained by the condition

$$\frac{\partial F(D)}{\partial D_{l,i}} = 0 \qquad (l = 1,2,...,M,\ j = 1,2,...,J) \tag{4}$$

Equation (4) generates $M \times J$ nonlinear equations, and the solution process must ensure that all $D_{m,j}$ are real and positive. Theoretically, $J \leqslant M$ sound sources can be solved, but the stability of the system is very poor, and the cross spectrum of microphone signals with high separation and poor correlation may also have problems. Therefore, additional conditions are needed to solve it. Michel[14,15] assumed that the directivities of neighbouring source positions are very similar. It can be described by the following two functions

$$G_1(D) = \sum_{j=1}^{J} \sum_{m=2}^{M-1} \left(D_{m,j} - 0.5\left(D_{m-1,j} + D_{m+1,j} \right) \right)^2 \tag{5}$$

$$G_2(D) = \sum_{j=2}^{J-1} \sum_{m=1}^{M} \left(D_{m,j} - 0.5\left(D_{m,j-1} + D_{m,j+1} \right) \right)^2 \tag{6}$$

The solution of Equation (3) is finally transformed into the solution of the following equation

$$\frac{\partial G(D)}{\partial D_{m,j}} = \frac{\partial F(D)}{\partial D_{m,j}} + \sigma_1 \frac{\partial G_1(D)}{\partial D_{m,j}} + \sigma_2 \frac{\partial G_2(D)}{\partial D_{m,j}} = 0 \tag{7}$$

where σ1 and σ2 are slack variables, and they have to be optimised experimentally.

Finally, it needs to solve the following nonlinear equations

$$\left\{\begin{aligned} &4\sum_{m=1}^{M} D_{m,i}(g_{l,i}g^{*}_{\mathrm{m},i}(\Gamma^{mes}_{l,m}-\sum_{j=1}^{J}(g_{l,j}D_{l,j}D_{m,j}g^{*}_{m,j}))) \\ &+\sigma_1(0.5D_{l,i\text{-}2}-2D_{l,i\text{-}1}+3D_{l,i}-2D_{l,i+1}+0.5D_{l,i+2}) \\ &+\sigma_2(0.5D_{l-2,i}-2D_{l-1,i}+3D_{l,i}-2D_{l+1,i}+0.5D_{l+2,i}) \end{aligned}\right\}=0 \quad (l=1,2,...,M, i=1,2,...,J) \tag{8}$$

This is a huge set of nonlinear equations with poor stability and long calculation time. The Quasi-Newton method [22,23,24] can be used to solve Equation (8).

In order to ensure that the solution result is positive, DLR minimize the squares of the directivities such that the directivities are automatically positive. $D_{m,j}$ is replaced by

$$D_{m,j}=d^2_{m,j} \tag{9}$$

At present, the latest SODIX version presents an updated version of the method that includes an optimized initial guess, a new convergence criterion, and a state-of-the-art solver in the minimization process. In this specific application with 248 microphones in the array, the computational time is reduced from 130 hours with the previous version to only 3.5 hours with the new SODIX version [20]. However, higher computing resources are still required.

In this paper, SODIX-Bes method based on beamforming and SODIX method is developed in order to further save computational time. The method can be calculated using a personal computer and takes less time. The next section will describe the SODIX-Bes method.

2.2 SODIX-Bes method

2.2.1 Sound power spectrum matrix of the microphone array based on Clean-SC

Assuming that a microphone array is used for experimental measurement, the total number of microphones in the array is M, and the sound pressure signal received by microphone m is $p^{mes}_m(t)$, then CSM of all microphone signals $p^{mes}_m(t)$ (m=1, 2, …, M) is defined by

$$C^{mes}(f)=\begin{bmatrix} C^{mes}_{1,1}(f) & \cdot & C^{mes}_{1,M}(f) \\ \cdot & \cdot & \cdot \\ C^{mes}_{M,1}(f) & \cdot & C^{mes}_{M,M}(f) \end{bmatrix} \tag{10}$$

Where, $C^{mes}(f)$ is CSM at frequency f.

The iterative formula of the CLEAN-SC algorithm [10] based on the spatial coherence of sound sources is

$$\left\{\begin{aligned} O^{(i)} &= \varphi Y^{(i-1)}_{\max}\Phi(\mathbf{x}-\mathbf{x}^{(i-1)}_{\max}) \\ Y^{(i)} &= \boldsymbol{\xi}^{*}\cdot\mathbf{D}^{(i)}\cdot\boldsymbol{\xi} \\ \mathbf{D}^{(i)} &= \mathbf{D}^{(i-1)}-\varphi Y^{(i-1)}_{\max}\left(\mathbf{h}^{*(i-1)}\mathbf{h}^{(i-1)}\right) \end{aligned}\right. \tag{11}$$

$$Z=\sum_{i=1}^{I}O^{(i)}+Y^{(I)} \tag{12}$$

Where, $Y^{(i)}_{\max}$ is the peak point in sound source maps; Φ is the beam function after normalization, $\Phi(0)=1$; $\xi=g/\mathrm{M}$; $\mathbf{D}^{(i)}$ is the cross spectral matrix after degradation, $\mathbf{D}^{(0)}$=CSM; $\varphi(0<\varphi<1)$ is the safety factor; **h** is the component of a single relevant sound source. **Z** is the final sound source distribution map.

Based on the iterative process of the CLEAN-SC algorithm, we can also obtain $\mathrm{CSM}^{\text{Clean-SC}}$ that eliminates large sidelobe information

$$\mathrm{CSM}^{Clean-SC} = \sum_{i=1}^{I} \varphi Y_{\max}^{(i)} \left(\mathbf{h}^{*(i)} \mathbf{h}^{(i)} \right) + \mathrm{D}^{(I)} \tag{13}$$

Let,

$$C^{SC} = \mathrm{CSM}^{Clean-SC} \tag{14}$$

Then,

$$C^{SC}(f) = \begin{bmatrix} C_{1,1}^{SC}(f) & \cdot & C_{1,M}^{SC}(f) \\ \cdot & \cdot & \cdot \\ C_{M,1}^{SC}(f) & \cdot & C_{M,M}^{SC}(f) \end{bmatrix} \tag{15}$$

The master diagonal of Equation (15) constitutes the noise power spectrum matrix of the microphone signals is defined by

$$C_{m,m}^{SC}(f) = \begin{bmatrix} C_{1,1}^{SC}(f) \\ \vdots \\ C_{m,m}^{SC}(f) \end{bmatrix} \qquad m = 1, 2, \ldots, M \tag{16}$$

Let,

$$W_{m,l}^{SC} = C_{m,m}^{SC}(f) \tag{17}$$

Where l is the l-th frequency on the spectrum line. For example, frequency range of the spectrum is 0 Hz-16384 Hz, and the interval of the frequency is 32 Hz, then 3200 Hz is the 101st frequency, l=101 at this time.

The noise power spectrum matrix of the microphone signals for all frequencies is defined by

$$\boldsymbol{W}_{M,L}^{SC} = \begin{Bmatrix} C_{1,1}^{SC}(f_1) & \cdot & C_{1,1}^{SC}(f_L) \\ \cdot & \cdot & \cdot \\ C_{M,M}^{SC}(f_1) & \cdot & C_{M,M}^{SC}(f_L) \end{Bmatrix} = \begin{Bmatrix} W_{1,1}^{SC} & \cdot & W_{M,L}^{SC} \\ \cdot & \cdot & \cdot \\ W_{M,1}^{SC} & \cdot & W_{M,L}^{SC} \end{Bmatrix} \tag{18}$$

Where L is the total number of frequencies on the spectrum.

At the same time, we can also obtain the number, position and spectral information $S_j(f)$ of major sound sources from the beamforming map by Equation (11). The SODIX-Bes method is to fit the measured signal and the model signal containing the main sound source information to obtain the sound source directivity.

2.2.2 Noise power spectrum matrix of the model signals

Since $S_j(f)$ is known, it can be further assumed that the directivity function of the microphone m to the sound source j is $d_{m,j}$, then Equation (1) can be transformed into

$$C_{m.n}^{\mathrm{mod}}(f_l) = \sum_{j=1}^{J} g_{m,j} S_j(f_l) d_{m,j} d_{n,j} g_{n,j}^{*} \tag{19}$$

Since each sound source has a fixed direction angle $\theta_{m,j}$ relative to each microphone. Therefore, for a microphone m at a fixed position in the microphone array, the goal of this paper is to determine the directivity function $D(\theta_{m,j})$ of J sound sources

$$C_{m.m}^{\mathrm{mod}}(f_l) = \sum_{j=1}^{J} g_{m,j} S_j(f_l) D(\theta_{m,j}) g_{m,j}^{*} \tag{20}$$

All elements of Equation (20) constitute the noise power spectrum matrix of the model microphone signals

$$C_{m,m}^{\mathrm{mod}}(f_l)=\begin{bmatrix} C_{1,1}^{\mathrm{mod}}(f_l) \\ \vdots \\ C_{m,m}^{\mathrm{mod}}(f_l) \end{bmatrix} \qquad m=1,2,\ldots,M \tag{21}$$

Let

$$W_{m,l}^{\mathrm{mod}}=C_{m,m}^{\mathrm{mod}}(f_l)=\sum_{j=1}^{J} g_{m,j}S_j(f_l)D(\theta_{m,j})g_{m,j}^{*} \tag{22}$$

The noise power spectrum matrix of the microphone signals for all frequencies is defined by

$$\boldsymbol{W}_{M,L}^{\mathrm{mod}}=\begin{Bmatrix} C_{1,1}^{\mathrm{mod}}(f_1) & \cdot & C_{1,1}^{\mathrm{mod}}(f_L) \\ \cdot & \cdot & \cdot \\ C_{M,M}^{\mathrm{mod}}(f_1) & \cdot & C_{M,M}^{\mathrm{mod}}(f_L) \end{Bmatrix}=\begin{Bmatrix} W_{1,1}^{\mathrm{mod}} & \cdot & W_{1,L}^{\mathrm{mod}} \\ \cdot & \cdot & \cdot \\ W_{M,1}^{\mathrm{mod}} & \cdot & W_{M,L}^{\mathrm{mod}} \end{Bmatrix} \tag{23}$$

2.2.3 Determination of the directivities of the sources

The ultimate purpose of this paper is to determine the directivity $D(\theta_{m,i})$ of the sources j toward the microphone m, such that the mean square error $F(D(\theta))$ between $W_{m.l}^{SC}$ and $W_{m.l}^{\mathrm{mod}}$ is minimum.

$$F\left(D\left(\theta_{m,j}\right)\right)=\sum_{m=1}^{M}\left|W_{m,l}^{SC}-W_{m,l}^{\mathrm{mod}}\right|^2=\sum_{m=1}^{M}\left|W_{m,l}^{SC}-\sum_{j=1}^{J}g_{m,j}S_j(f_l)D(\theta_{m,j})g_{m,j}^{*}\right|^2 \tag{24}$$

In order to minimize the fitting error, Equation 24 can be transformed into

$$\frac{\partial F\left(D\left(\theta_{m,j}\right)\right)}{\partial D\left(\theta_{m,j}\right)}=0 \tag{25}$$

That is,

$$W_{m,l}^{SC}\left(f_l\right)=\sum_{i=1}^{J}g_{m,i}S_i\left(f_l\right)D\left(\theta_{m,i}\right)g_{m,i}^{*} \tag{26}$$

Assume

$$A_{m,l}=W_{m,l}^{SC}\left(f_l\right) \tag{27}$$

$$B_{m,l}=\sum_{i=1}^{J}g_{m,i}S_i\left(f_l\right)D\left(\theta_{m,j}\right)g_{m,i}^{*} \tag{28}$$

Then the error Equation (26) can be expressed as

$$\begin{bmatrix} A_1(f_1) & A_1(f_2) & \cdots & A_1(f_L) \\ A_2(f_1) & A_2(f_2) & \cdots & A_2(f_L) \\ \vdots & \vdots & & \vdots \\ A_M(f_1) & A_M(f_2) & \cdots & A_M(f_L) \end{bmatrix}=\begin{bmatrix} B_1(f_1) & B_1(f_2) & \cdots & B_1(f_L) \\ B_2(f_1) & B_2(f_2) & \cdots & B_2(f_L) \\ \vdots & \vdots & & \vdots \\ B_M(f_1) & B_M(f_2) & \cdots & B_M(f_L) \end{bmatrix} \tag{29}$$

Equation (29) is an $M\times L$ order linear equation system about the number of sound source spectral lines L and the number of microphones M, and the equation system contains $M\times J$ unknowns. Because L is usually much larger than J, the equations are benign. Meanwhile, the solution result must be a positive value. It can be solved by least square method, so as to obtain the directivity function $D(\theta_{m,i})$ of each sound source.

3 COMPUTER SIMULATION

In order to verify the effectiveness of the method developed in this paper, computer simulation experiments are firstly carried out. Figure 1 shows the test set-up for the computer simulation.

As shown in Figure 1, the sound source simulation experiment applied a linear array of 15 microphones, and the centre coordinate of the array is: (0 m, 0 m, 0 m), and two sound sources were simulated. The coordinate of sound source 1 is: (-0.3 m, 0 m, 2 m), the coordinate of sound source 2 is: (0.3 m, 0 m, 2 m). The definition of the direction angle θ is also shown in Figure 1.

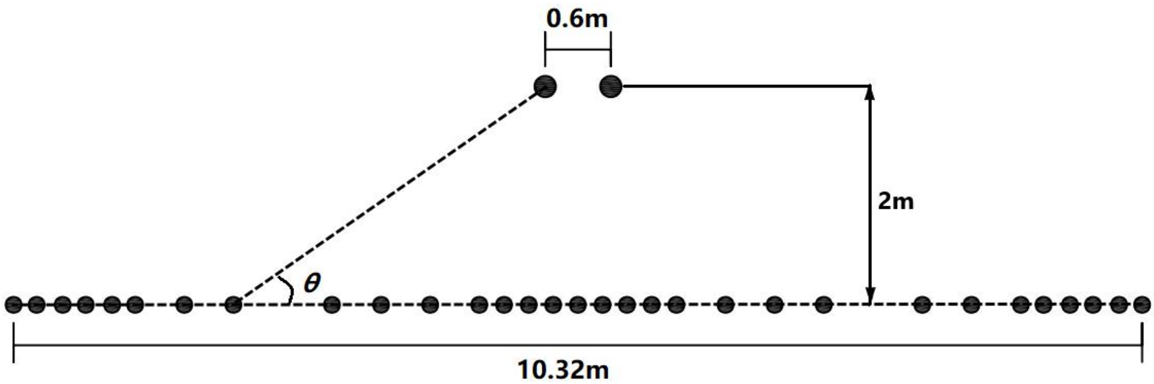

Fig. 1. The computer simulation

The sound pressure level of the two simulated sound sources is 90 dB, and the frequencies are 2950 Hz and 3050 Hz. The sound signals of the simulated sound sources are spherical waves (that is the spherical directivity). The sampling frequency of the microphone array is 32768 Hz, and the sampling time is 15 s. During data processing, the number of Fourier transform points is 2048, and the Hanning window is applied in FFT calculation, the data is segmented and averaged multiple times, and there is a 50% overlap between two adjacent segments of data. The normalized spectrum of sound source can be obtained by beamforming.

First, the results of SODIX method are obtained (The results were taken from 15 of the 31 microphones). Figure 2 shows the nonlinear iterative process of SODIX method. Figure 3 shows the comparison between the calculation results of SODIX method and the theoretical results. The theoretical results are the results of separate simulation of two sound sources at the same coordinate position.

As can be seen Figure 2 and Figure 3, it takes 270.04 s to converge by SODIX. This is only the calculation time of 15 microphones and two sound sources. It can be predicted that if the number of microphones and sound sources increases, the calculation time will increase explosively.

In contrast, since the SODIX-Bes method transforms the solution of the nonlinear equation system into the solution of the linear equation system, there is no complex nonlinear iteration. With the same computer, the SODIX-Bes method takes only 9.37 s to obtain the results shown in Figure 4. Compared with SODIX method, SODIX-Bes method has higher computational efficiency. It can be seen from Figure 4 that the SODIX-Bes results agree well with the theoretical results.

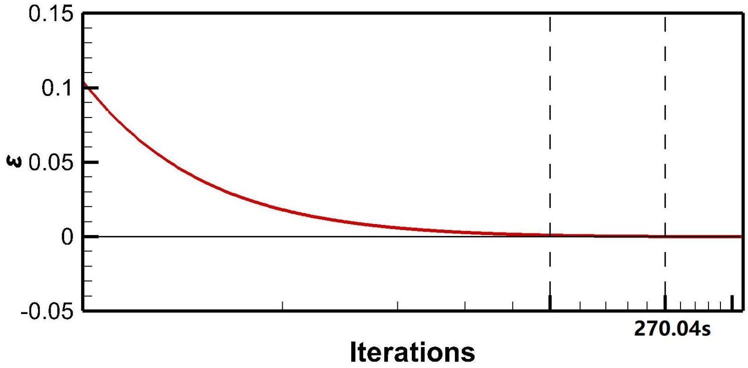

Fig. 2. Iterative process of SODIX

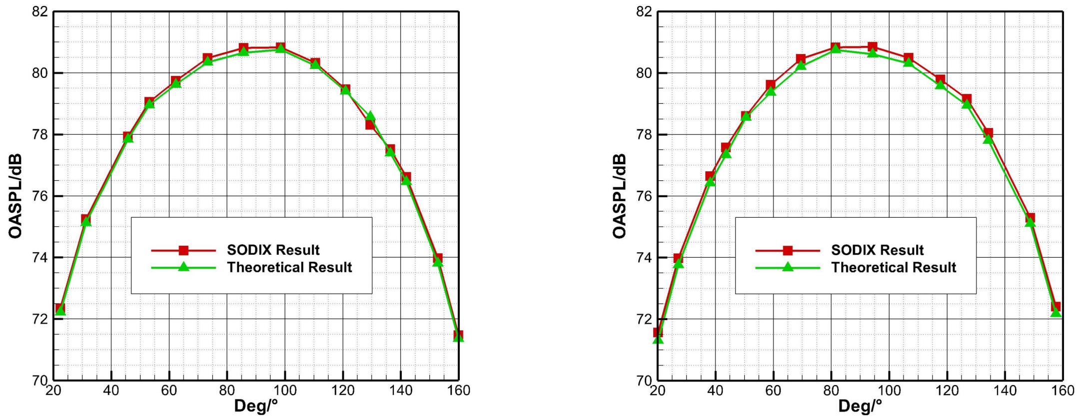

(*a*) *Source 1* (*b*) *Source 2*

Fig. 3. The comparison between the SODIX results and the theoretical results

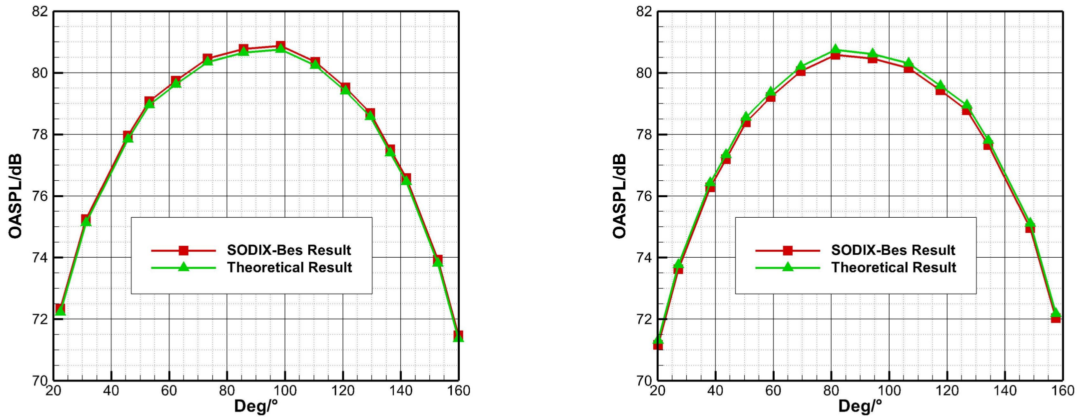

(*a*) *Source 1* (*b*) *Source 2*

Fig. 4. The comparison between the SODIX-Bes results and the theoretical results

Figure 5 is the errors between the SODIX-Bes results and the theoretical results. It can also be concluded from Figure 5 that the error value between the SODIX-Bes results and the theoretical results does not exceed 0.17 dB at most, when the two sound sources are simulated by computer. This shows that the SODIX-Bes method has a high accuracy in solving the directivity of multiple sound sources. The SODIX-Bes method can be calculated on a personal computer.

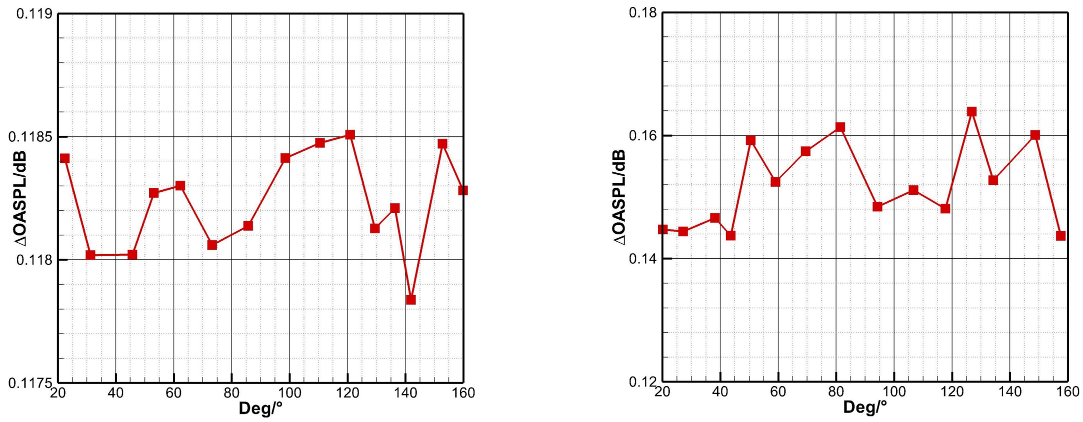

(*a*) *Source 1* (*b*) *Source 2*

Fig. 5. The errors between the SODIX-Bes result and the theoretical result

4 THE IDENTIFICATION OF THE DIRECTIVITY OF LEADING-EDGE NOISE WITH SODIX-BES

4.1 Experiment set-up

The blade leading-edge(LE) noise test was carried out in the low speed open jet wind tunnel in Northwestern Polytechnical University(NPU), and the NACA65(12)-10 blade is tested. The test blade is with a chord of 150 mm and a span of 300 mm. In the experiment, the wavy leading edge is used to reduce the noise of the blade leading edge. Figure 6 shows the definitions of the wavy amplitude (*A*) and wavelength (*W*) for the wavy blades. A total of 3 wavy LE blades, as shown in Table 1, were designed and tested in this experiment. Table 1 gives the design parameters of the wavy LE blades. In this table, *c* means the chord of the blade.

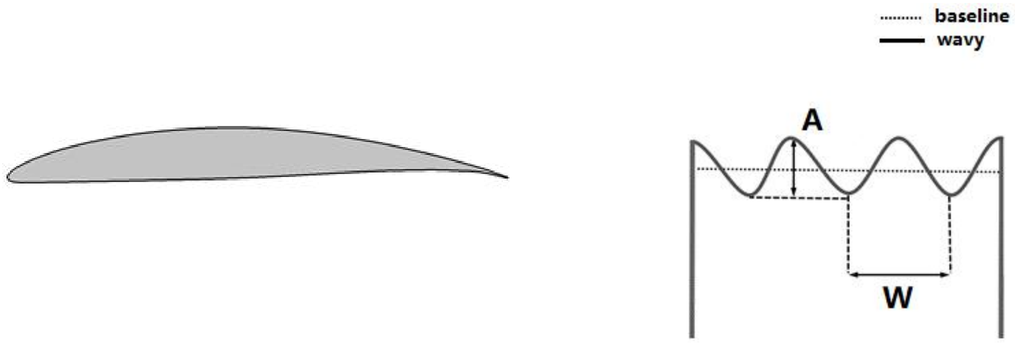

Fig. 6. NACA65(12)-10 blade and wavy leading-edge

Table. 1. Design parameters of the wavy LE configuration

	A/c	*W/c*
baseline	0	0
A5W20	0.05	0.2
A10W20	0.10	0.2
A30W20	0.30	0.2

Figure 7 shows the test set-up. The blade was placed into the core of the open jet of the wind tunnel exit. The blade is mounted onto a plexiglass disk as shown in Figure 8(a), which allows tuning the angle of attack. The angle of attack in this paper is 0°. The wind tunnel has a rectangular exit with dimensions of 0.3 m × 0.09 m. The maximum inflow velocity is 100 m/s with turbulence intensity below 1%. The uncertainty of the inlet mean velocity is within

0.5%. As shown in Figure 8(b), a linear array with 31 microphones and with nonuniform distribution in length 1.72 m was used in the study. The array is 0.66 m below the test blade with the array center located at the mid-chord of the blade. The microphones are installed on a board surface. θ is the direction angle. The outlet velocity of the wind tunnel is 83.6 m/s.

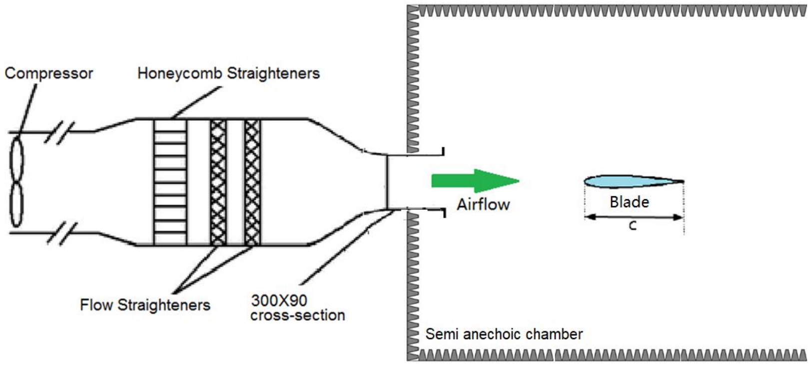

Fig. 7. Test set-up

(*a*) *Test Blade*

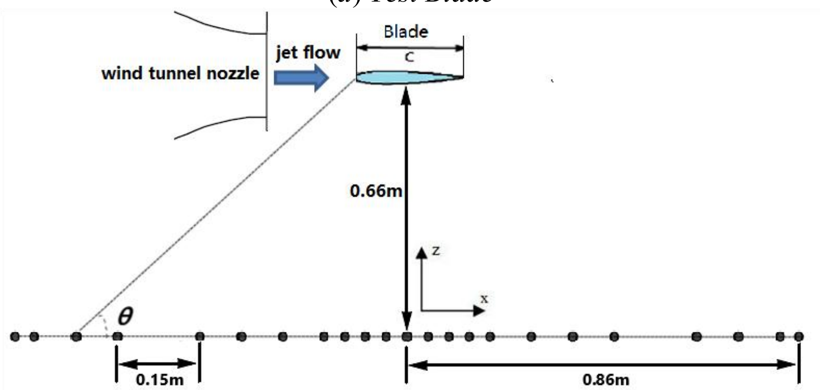

(*b*) *Microphone array*

Fig. 8. Test blade and Microphone array

The 1/4 inch BSWA microphones are utilized in the experiment. All the microphones are calibrated by a standard noise source with a frequency of 1000 Hz and a SPL of 94 dB. The acoustic time signals are recorded with a sampling rate of 32,768 Hz for 15 s. Data were processed with a Hanning window of 50% overlap and a frequency resolution of 16 Hz.

4.2 Noise Sources Identification

The beamforming based on Clean-SC was firstly used to identify the blade noise sources. Figure 9 shows the sound source identification maps of different wavy amplitudes under the flow condition of U = 83.6 m/s and with wavy wavelength W= 20 mm.

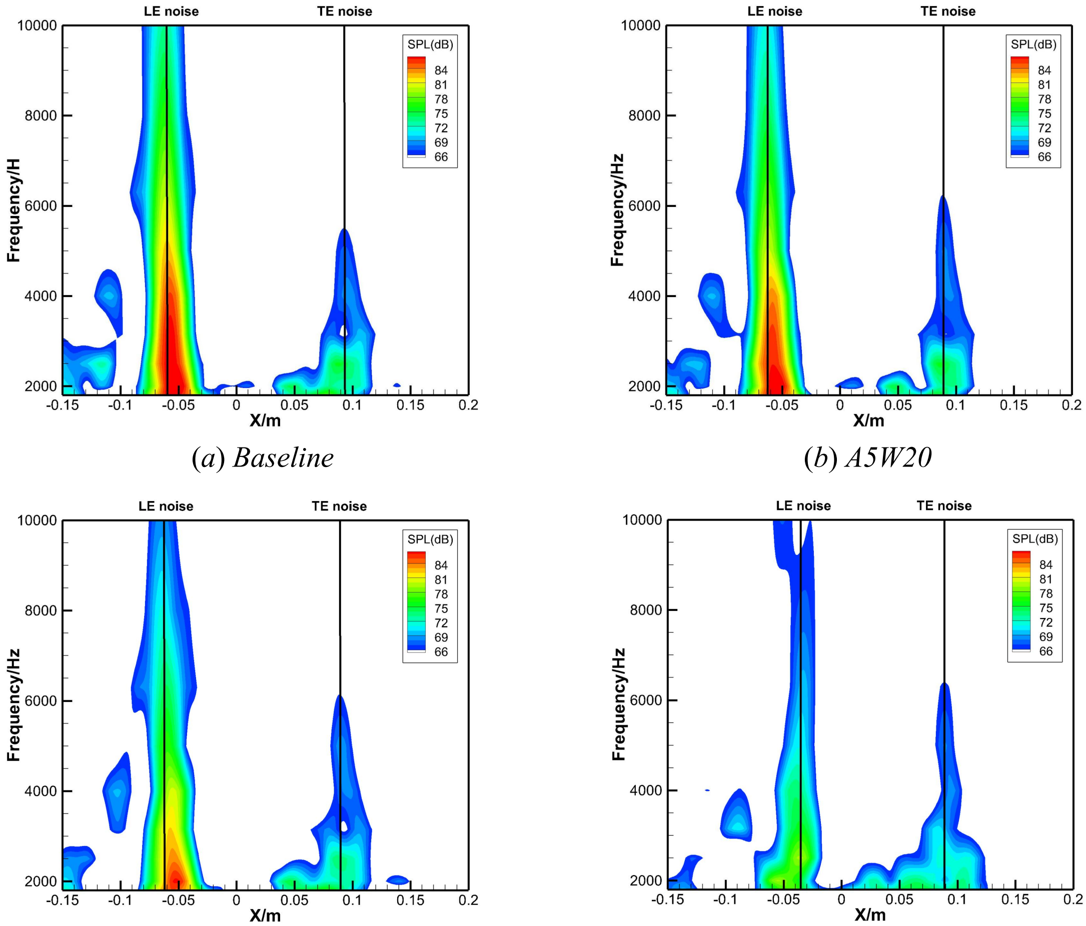

(*a*) *Baseline* (*b*) *A5W20*

(*c*) *A10W20* (*d*) *A30W20*

Fig. 9. The sound source distribution of the blade with different wavy amplitudes ($U = 83.6$ *m/s*).

It can be seen from the Figure 9 that both the leading-edge (LE) noise and trailing-edge (TE) noise sources can be separated correctly, and the LE noise can be significantly reduced with the wavy treatment. And it can be seen from the beamforming results that as the amplitude increases, the reduction of the LE noise is increasing, and the position of the LE noise also changes. At the same time, it has also some impact on the TE noise.

4.3 Spectral analysis

It could be seen from the beamforming results that the main lobes of LE and TE noise all have some width in space. The magnitude of the LE and TE noise should be the sum of sound level in specified space. In this paper, the sound pressure levels of LE noise are evaluated using the following equation:

$$L = 10\lg\left(\frac{\sum_{n=N_{\min}}^{N_{\max}} 10^{0.1L_n}}{N_{\max} - N_{\min} + 1}\right) \tag{30}$$

Suppose that the LE noise source center is at the position of maximum overall sound pressure level OASPL, $N_{\min}$ and $N_{\max}$ are, respectively, the upstream and downstream positions where the OASPL is 3 dB smaller than the maximum OASPL. L_n is the sound pressure level at the position n.

Figure 10 shows the spectrum and the 1/3 octave spectra of the LE noise (1600 Hz-10000 Hz) for the blade with different LE wave at airflow speeds of 83.6 m/s. It can be seen from Figure 10 that the wavy LE can effectively reduce the LE noise. From Figure 10(a), it can be seen that when the wavelength is constant, the noise reduction of four different amplitude blades is 2-10 dB at airflow speeds of 83.6 m/s, and the reduction of the LE noise increases with the increase of the amplitude. Figure 10(b) shows that the noise reduction of A30W20 blades below 6000Hz is more significant than that above 6000Hz.

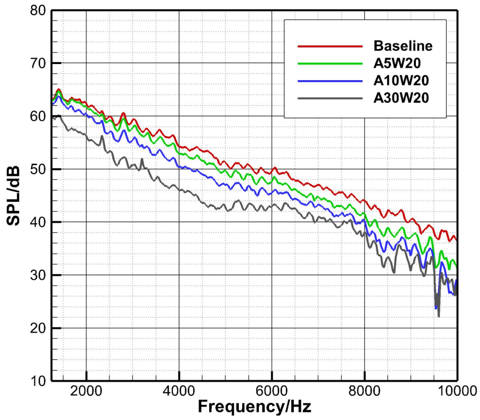

(*a*) *The spectrum*

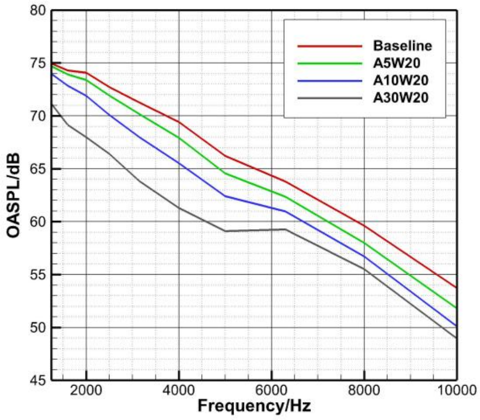

(*b*) *The 1/3 octave spectra*

Fig. 10. Spectra of the LE noise with different wavy amplitudes (*U=83.6 m/s*, *W=20 mm*)

4.4 The identification of the directivity of leading-edge noise based on SODIX-Bes and comparison with the theoretical function model

In this section, the directivity results of the LE noise of normal leading-edge based on SODIX-Bes are compared with the theoretical function model. Figure 11 shows the parameter definition. Equation (31) and Equation (32) are directivity functions of the LE noise for the low and high frequency [25].

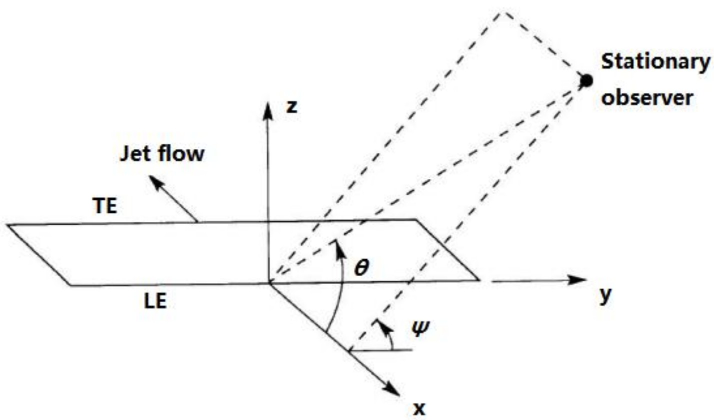

Fig. 11. Parameter definition

$$D_l(\theta,\psi) \approx \frac{\sin^2\theta \sin^2\psi}{(1+M\cos\theta)^4} \qquad (\mathit{frequency} \leqslant 5000Hz) \tag{31}$$

$$D_h(\theta,\psi) \approx \frac{2\sin^2(\theta/2)\sin^2\psi}{(1+M\cos\theta)[1+M\cos\psi]^2} \quad (frequency > 5000Hz) \tag{32}$$

Where, θ is the direction angle in X-axis direction, Ψ is the direction angle in Y-axis direction (In this paper, Ψ=90°), M is the Mach number of airflow.

Figure 12 shows the comparison between experimental results based on SODIX-Bes and theoretical function model of the LE noise at airflow speeds of 83.6 m/s, 2000 hz-3000 Hz and 7000Hz-8000Hz. The 2000Hz-3000Hz directivity function results are the results of Equation (31). The 7000Hz-8000Hz directivity function results are the results of Equation (32). The sound pressure level of the LE noise predicted theoretically is normalized by the results of Beamforming.

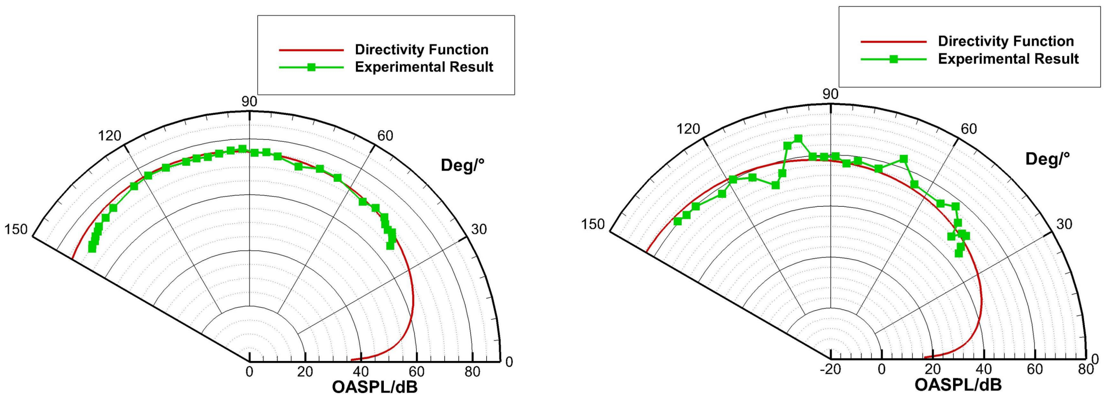

(*a*) *2000 Hz-3000 Hz* (*b*) *7000 Hz-8000 Hz*

Fig. 12. The directivity of the LE noise (*U=83.6 m/s*)

It can be seen from Figure 12(a), at 2000 hz-3000 Hz, the SODIX-Bes results are in good agreement with the theoretical function model; and it can be seen in Figure 12(b), the directivity of the LE noise shows an obvious burr shape at 7000hz-8000hz, but the SODIX-Bes results still fluctuate up and down around the theoretical function model. This is because the directivity function is simplified in theoretical function. According to Renzo Arina and Andrea Ferrero[26], when the frequency is 100 Hz, the shape of the trailing-edge noise has the dipole characteristics as shown in Figure 13(a). However, with the increase of frequency, the directivity of the trailing-edge noise presents the burr shape as shown in Figure 13(b). According to the theory of Amiet[27], the directivity of the leading-edge noise will have a similar situation. By comparing the experimental results based on SODIX-Bes with the theoretical function model, it can be seen that the SODIX-Bes method can accurately capture the directional characteristics of the LE noise.

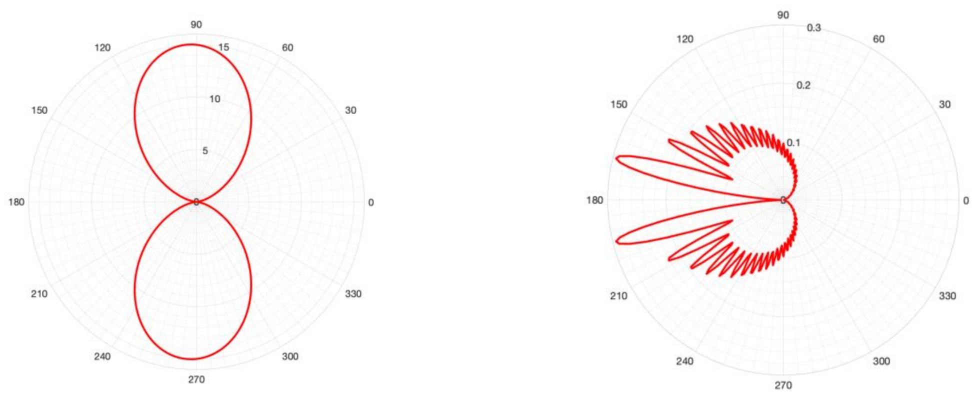

(*a*) *100Hz* (*b*) *10000Hz*

Fig. 13. The directivity of the LE and TE noise

4.5 The reduction of the leading-edge noise with wavy configuration

Figure 14 shows the comparison of directivity results(1600Hz-10000Hz) of the LE noise of the straight LE and wavy LE blade based on SODIX-Bes at airflow speeds of 83.6 m/s.

From Figure 14, it can be seen that all wavy blades have noise reduction at the radiation angles of 40°-140° at airflow speed of 83.6 m/s. The noise reduction effect of A5W20 blade is relatively uniform at the direction angle of 40° to 140°, the reduction of noise is 1 to 3 dB. A10W20 blade has more noise reduction at the direction angle of 75° to 85°, the maximum reduction of noise is 9.05 dB. The noise reduction of A30W20 blade is more significant, especially the direction angle of 100° to 140°, the radiation intensity of the LE noise is greatly reduced. In general, the radiation intensity of the LE noise decreases with the increase of the wavy amplitude at the direction angle of 40° to 140°.

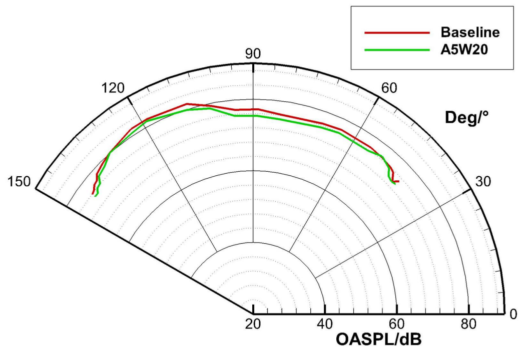

(a) A5W20

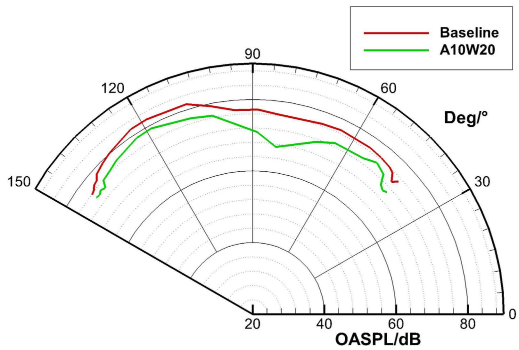

(b) A10W20

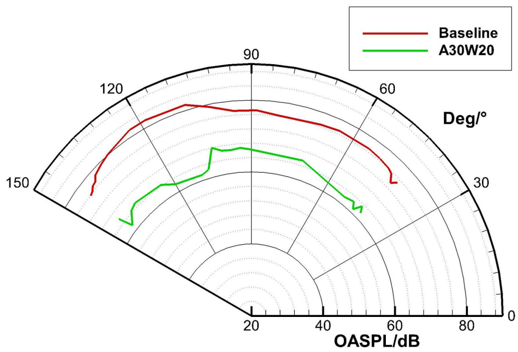

(c) A30W20

Fig. 14. The LE noise directivity of the blade with different wavy amplitudes (U = 83.6 m/s, W = 20 mm)

4.6 Reduce the influence of background noise

The main diagonal of CSM is greatly affected by the background noise. We use the M-1 elements close to the main diagonal shown in Equation (33) for the directivity solution, at this time we can obtain an average directivity for m+1 and m microphones.

$$C_{m+1,m}^{mes}(f)=\begin{bmatrix} C_{2,1}^{mes}(f) \\ C_{3,2}^{mes}(f) \\ \vdots \\ C_{M,M-1}^{mes}(f) \end{bmatrix} \tag{33}$$

$W_{m,l}$ is replaced by

$$W_{m,l} = \begin{bmatrix} C_{2,1}^{mes}(f_1) & C_{2,1}^{mes}(f_2) & \cdots & C_{2,1}^{mes}(f_L) \\ C_{3,2}^{mes}(f_1) & C_{3,2}^{mes}(f_2) & \cdots & C_{3,2}^{mes}(f_L) \\ \vdots & \vdots & & \vdots \\ C_{M,M-1}^{mes}(f_1) & C_{M,M-1}^{mes}(f_2) & \cdots & C_{M,M-1}^{mes}(f_L) \end{bmatrix} \tag{34}$$

Finally solve Equation (35)

$$F\left(D\left(\theta_{m,j}\right)\right) = \sum_{m=1}^{M-1} \left| W_{m,l} - W_{m,l}^{\text{mod}} \right|^2 = 0 \tag{35}$$

The equation is equivalent to solving a system of equations for M-1 microphones and J sound sources. Figure 15 shows the comparison between the solution results (1600Hz-10000Hz) of Equation (36) and that of Equation (24). In Figure 15, No. 1 is the results of Equation (24), and No. 2 is the results of Equation (36). It can be seen from the figure that the directivity results calculated by the two equations are in good agreement.

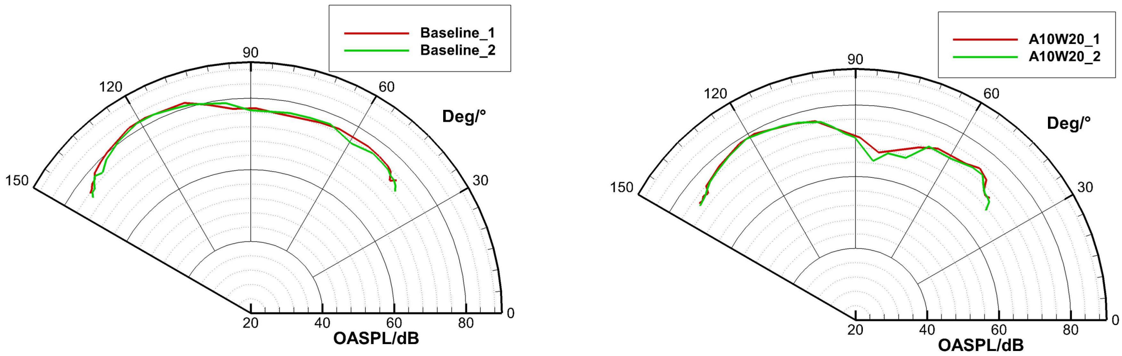

(*a*) *Baseline* (*b*) *A10W20*

Fig. 15. the comparison of the LE noise directivity

CONCLUSION

An extended SODIX, SODIX-Bes, for the identification of the directivity of flow noise source was proposed and developed in this paper. Using the computing simulation, the SODIX-Bes method is verified. The calculation simulation results show that the maximum error of SODIX-Bes method is no more than 0.17 dB. The SODIX-Bes was used in this study to investigate the noise reduction effect of the wavy leading-edge blades. Clear and quantitative sound radiation results from the LE noise source were obtained, and the influence of the wavy LE blades on the directivity of the LE noise are obtained. The study of the directivity of the LE noise shows that different wavy LE have noise reduction effects at different radiation angles, and the radiation intensity of the LE noise decreases with the increase of the wavy amplitude.

The results of computer numerical simulation and blade leading-edge noise experiment show that the SODIX-Bes developed in this paper has good performance of accurately identifying the intensity and directivity of noise source. Compared with SODIX method, SODIX-Bes method saves a lot of computation time, and it does not need too many computing resources, can be calculated on a personal computer.

ACKNOWLEDGEMENTS

The present work is supported by the National Natural Science Foundation of China (Project Grant No.51936010), and Supported by National Science and Technology Major Project (2017-II-0008-0022).

The author would like to especially thank Professor U. Michel, the initiator of SODIX method. The author had a very useful exchange and discussion with Professor Michel on the matching of CSM, and Prof. Michel gave author specific detailed comments on present research work.

REFERENCES

[1] J. Billingsley. “An acoustic telescope: ARC 35/364.” Aeronautical Research Council, 1974.

[2] J. Billingsley and R. Kinns. “The acoustic telescope.” Journal of Sound and Vibration, 48, (1976), pp. 485-510.

[3] H. Siller. "Sound source localization with microphone arrays." Seminar des Northwestern Polytechnical University DLR, 2011.

[4] D. H. Johnson and D. E. Dudgeon. “Array signal processing: Concepts and techniques.” New Jersey: PTR Prentice Hall, 1993.

[5] R. P. Dougherty and R. W. Stoker. “Sidelobe suppression for phased array aeroacoustic measurements.” 4th AIAA/CEAS Aeroacoustics Conference, Toulouse, France, June 2-4, 1998.

[6] T. F. Brooks and W.M. Humphreys. “A deconvolution approach for the mapping of acoustic sources (DAMAS) determined from phased microphone arrays.” 10th AIAA/CEAS Aeroacoustics Conference, Manchester, UK, May 10–12, 2004.

[7] T. F. Brooks and W.M. Humphreys. “Three-dimensional application of DAMAS methodology for aeroacoustic noise source definition.” 11th AIAA/CEAS Aeroacoustics Conference, May 23–25, 2005, Monterey, California, USA, May 23–25, 2005.

[8] T. F. Brooks and W.M. Humphreys. “A deconvolution approach for the mapping of acoustic sources (DAMAS) determined from phased microphone arrays.” Journal of Sound and Vibration, 2006(294):856-879.

[9] R. P. Dougherty. “Extensions of DAMAS and benefits and limitations of deconvolution in beamforming.” 11th AIAA/CEAS Aeroacoustics Conference, Monterey, California, USA, May 23–25 2005.

[10] P. Sijtsma. “CLEAN based on spatial source coherence.” Int. J. Aeroacoust. 6(4), 357–374 (2007).

[11] G. P. Howell, A. J. Bradley, and M. A. McCormick. "De-Dopplerisation and acoustic imaging of aircraft flyover measurements." AIAA Journal -1(1984).

[12] U. Michel and W. Y. Qiao. “Directivity of landing-gear noise based on flyover measurements.” 5th AIAA/CEAS Aeroacoustics Conference, Bellevue, Greater Seattle, WA, USA, May 10–12 1999.

[13] H. A. Siller, F. Arnold and U. Michel. “Investigation of aero-engine core-noise using a phased microphone array.” 7th AIAA/CEAS Aeroacoustics Conference and Exhibit, Maastricht, Netherlands, May 28-30, 2001.

[14] U. Michel and S. Funke. “Noise source analysis of an aeroengine with a new inverse method SODIX.” 14th AIAA/CEAS Aeroacoustics Conference, Vancouver, BC, Canada, May 5–7, 2008.

[15] S. Funke, A. Skorpel and U. Michel. “An extended formulation of the SODIX method with application to aeroengine broadband noise.” 18th AIAA/CEAS Aeroacoustics Conference, Colorado Springs, USA, 4–6 June 2012.

[16] D. Blacodon and G. Elias. “Level Estimation of Extended Acoustic Sources Using an Array of Microphones.” Aiaa/ceas Aeroacoustics Conference. 2003.

[17] D. Blacodon and G. Elias. “Level Estimation of Extended Acoustic Sources Using a Parametric Method.” Journal of Aircraft, 2004.

[18] S. Funke, R. P. Dougherty and U. Michel. “SODIX in comparison with various deconvolution methods.” 5th Berlin Beamforming Conference, 2014.

[19] S. Oertwig, S. Funke and A. H. Siller. “Improving source localisation with SODIX for a sparse microphone array.” 7th Berlin Beamforming Conference, DLR, 2018.

[20] S. Oertwig, H. A. Siller and S. Funke. “Advancements in the source localization method SODIX and application to short cowl engine data.” 25th AIAA/CEAS Aeroacoustics Conference, Delft, The Netherlands, 20-23 May 2019.

[21] E. Sarradj. “An Inverse Microphone Array Method for the Estimation of a Rotating Source Directivity.” Acoustics 3(2021).

[22] W. C. Davidon. “Variable metric method for minimization.” AEC Res. and Dev. Report ANL-5990(1959).

[23] R. Fletcher and M. J. D. Powell. “A rapid convergent descent method for Minimization.” Computer Journal, 1963, 6:163-168.

[24] T. Steihaug. “Quasi-Newton methods for large scale optimization.” PH. D. Dissertation. SOM Technical Report No. 49, Yale University, 1984.

[25] T. F. Brooks, D. S. Pope and M. A. Marcolini. “Airfoil Self-Noise and Prediction. ” NASA Reference Publication 1218, July 1989.

[26] R. Arina and A. Ferrero. “Data-Driven Aeroacoustic Modelling: Trailing-Edge Noise.” Aiaa aviation forum, August 2-6, 2021.

[27] R. K. Amiet. “Acoustic radiation from an airfoil in a turbulent stream.” Journal of Sound and Vibration, 1975(41):407–420.